PHYSICAL REVIEW A **75**, 033411 (2007)

# Two-photon double ionization of helium in the region of photon energies 42–50 eV

I. A. Ivanov* and A. S. Kheifets
*Research School of Physical Sciences and Engineering, The Australian National University, Canberra ACT 0200, Australia*

(Received 19 November 2006; revised manuscript received 20 February 2007; published 23 March 2007)

We report the total integrated cross section (TICS) of two-photon double ionization of helium in the photon energy range from 42 to 50 eV. Our computational procedure relies on a numerical solution of the time-dependent Schrödinger equation on a square-integrable basis and subsequent projection of this solution on a set of final field-free states describing correlation in the two-electron continuum. Our results suggest that the TICS grows monotonically as a function of photon energy in the region of 42–50 eV, possibly reaching a maximum in the vicinity of 50 eV. We also present fully resolved triple-differential cross sections for selected photon energies.

DOI: 10.1103/PhysRevA.75.033411 PACS number(s): 32.80.Rm, 32.80.Fb, 42.50.Hz

## I. INTRODUCTION

Multiphoton atomic ionization resulting in ejection of a single electron, as well as other single active electron phenomena in intense laser fields, are relatively well understood by now [1]. In contrast, strong field ionization with several active electrons involved is a much more challenging problem in which the highly nonlinear field interaction is entangled with the few-body correlated dynamics [2]. Two-photon double-electron ionization (TPDI) of helium is the archetypal reaction of this kind. Even for this simplest many-photon many-electron process, nonperturbative treatment of the external field is essential as well as a proper account of correlation in the two-electron continuum. Neglect of either aspects of TPDI may results in a gross failure.

Because of the canonical importance of the TPDI of He, a large number of theoretical methods have been developed and applied to this problem recently. Among them are the lowest-order perturbation theory (LOPT) with correlated multichannel states [3], the many-electron many-photon theory [4], the *R*-matrix Floquet approach [5], and various time-dependent methods [6–14]. These studies allowed one to achieve considerable progress in understanding the qualitative features of the TDPI phenomenon in He. However, as far as a quantitative description of TDPI is concerned, the available theoretical results paint a somewhat controversial picture.

There is one cluster of results produced by several methods such as the time-dependent close-coupling (TDCC) [6,15], time-dependent basis [8], and *R*-matrix Floquet [5] methods, which agree with each other with a typical accuracy of ~40% in the interval of the photon energies of 40–47 eV. These results indicate that the total integrated cross section (TICS) of TPDI is a monotonously growing function of the photon energy.

On the other hand, the LOPT calculation [3] produced a TICS which was several times larger for photon energies near 45 eV and decreased slowly with photon energy in the interval of 43–47 eV. In a recent time-dependent *J*-matrix calculation, Foumouo *et al.* [13] reported a TICS which was close to the LOPT results of Ref. [3] but was a growing function of photon energy in the interval 40–52 eV, reaching a maximum at about 50 eV. In a very recent work [14], the authors of Ref. [3] performed a time-dependent calculation of a TICS with the same set of multichannel final states they used in their LOPT study and found their results close to those of Foumouo *et al.* [13]. This brief account shows that there is a certain degree of uncertainty in the quantitative description of TPDI and that the matter is far from closed.

One reason which might explain a considerable difference of TICS results obtained by various methods is a different representation of the final doubly ionized atomic state. In Ref. [6], for instance, the final state was represented by a product of two Coulomb waves, thus neglecting the final-state correlation completely. At the same time, the *R*-matrix Floquet calculation [5] and Refs. [3,13] used various correlated final-state wave functions. In Ref. [8], the authors took account of the correlations in the final state by means of perturbation theory.

Foumouo *et al.* [13] presented a thorough discussion of the effect of an incomplete account of the correlation in the final state on the computed TICS. They noted that if the final-state correlation was neglected, the TICS results might depend strongly on the picture (Schrödinger or interaction) one adopts to describe the ionization process. The difference in TICS values given by different pictures may be quite considerable.

However, the difference in the treatment of the correlations in the final state in various calculations does not fully account for the difference between the two clusters of theoretical TICS. For instance, the results of Ref. [6] agree well with those of Ref. [5], the former employing an uncorrelated final state whereas the latter is using a correlated final state.

In an attempt to resolve this controversy, we apply in the present work yet another technique to calculate the TICS of TPDI of helium for the photon energies in the interval of 42–50 eV. We use a method which we proposed recently for single-photon double- ionization studies [16]. The method is based on a numerical integration of the time-dependent Schrödinger equation (TDSE) with subsequent projection of the solution on a set of the field-free final states of the helium atom with both electrons in continuum.

---

*Corresponding author. On leave from the Institute of Spectroscopy, Russian Academy of Sciences. Electronic address: Igor.Ivanov@.anu.edu.au

An accurate description of those states is, by itself, a rather complicated problem which can be tackled in a number of various ways. In Refs. [17,18], the correlation in the final state was taken into account perturbatively. One can also employ the exterior complex scaling method [19–21] or use the complex Sturmian basis [22]. Such a basis was also used in the Refs. [13,23]. The hyperspherical *R*-matrix method with semiclassical outgoing waves [24] and various implementations of the close-coupling method [25–28] were also used in single-photon double-ionization studies.

In our earlier work [16], we proposed to use the so-called convergent close-coupling (CCC) expansion [29] to describe the field-free two-electron continuum in conjunction with a solution of the TDSE. In that paper we considered effect of the external dc electric field on the single-photon double-electron ionization of He. In the present work, we apply this method for the study of TPDI.

The paper is organized as follows. In the next section we give an outline of the theoretical procedure. Then we discuss the results we obtained for the integrated and fully differential cross sections of TPDI of helium. We conclude by making observation on the role of the atom-field interaction and the final-state correlation in TPDI process.

## II. THEORY

A detailed description of our method can be found in Ref. [16]. We shall present here only a brief description of the computational procedure. At the first step we solve numerically the TDSE for the helium atom in the presence of the external ac field:

$$i\partial\Psi/\partial t = \hat{H}\Psi, \tag{1}$$

where

$$\hat{H} = \hat{H}_0 + \hat{V}_{12} + \hat{H}_{\mathrm{int}}(t), \tag{2}$$

where the noninteracting Hamiltonian and the Coulomb interaction are, respectively,

$$\hat{H}_0 = \frac{\boldsymbol{p}_1^2}{2} + \frac{\boldsymbol{p}_2^2}{2} - \frac{2}{r_1} - \frac{2}{r_2}, \tag{3}$$

$$\hat{V}_{12} = \frac{1}{|\boldsymbol{r}_1 - \boldsymbol{r}_2|}. \tag{4}$$

The interaction with the external ac field is written in the length gauge:

$$\hat{H}_{\mathrm{int}}(t) = f(t)(\boldsymbol{r}_1 + \boldsymbol{r}_2)\cdot \boldsymbol{F}_{\mathrm{ac}} \cos \omega t. \tag{5}$$

Here $f(t)$ is a smooth switching function which is chosen in such a way that it is zero for $t=0$ and $t=6T$, where $T=2\pi/\omega$ is a period of the ac field. For $t\in(T,5T)$, $f(t)=1$, and for $t\in(0,T)$ it grows monotonously, so that $f(t)$ and its derivative are continuous. Analogously, for $t\in(5T,6T)$, $f(t)$ smoothly decays from 1 to zero. The total duration of the atom-field interaction is therefore $T_1=6T$.

The solution of the TDSE is sought in the form of expansion on a square-integrable basis:

$$\Psi(\boldsymbol{r}_1,\boldsymbol{r}_2,t) = \sum_j a_j(t) f_j(\boldsymbol{r}_1,\boldsymbol{r}_2). \tag{6}$$

Here

$$f_j(\boldsymbol{r}_1,\boldsymbol{r}_2) = \phi^N_{n_1 l_1}(r_1)\phi^N_{n_2 l_2}(r_2)|l_1(1)l_2(2)L\rangle, \tag{7}$$

where the notation $|l_1(1)l_2(2)L\rangle$ is used for bipolar harmonics. The radial orbitals in Eq. (7) are the so-called pseudostates obtained by diagonalizing the He$^+$ Hamiltonian in a Laguerre basis [27]:

$$\langle \phi^N_{nl}|\hat{H}_{\mathrm{He}^+}|\phi^N_{n'l'}\rangle = E_i\delta_{nn'}\delta_{ll'}. \tag{8}$$

In the present work, we consider an electric field of the order of 0.1 a.u. corresponding to $3.5\times10^{14}$ W/cm$^2$ intensity. For this not very high field intensity, we can retain in the expansion (6) only terms with total angular momentum $J=0-2$. To represent each total angular momentum block, we proceed as follows. For all *S*, *P*, and *D* total angular momentum states we let $l_1$ and $l_2$ vary within the limits 0–3. The total number of pseudostates participating in building the basis states was 20 for each $l$. To represent $J=0,1,2$ singlet states in expansion (6), we used all possible combinations of these pseudostates. Such a choice gave us 840 basis states of *S* symmetry, 1200 basis states of *P* symmetry, and 1430 states of *D* symmetry, resulting in a total dimension of the basis equal to 3470. Issues related to the convergence of the calculation with respect to the variations of the composition of the basis set are described in detail in Ref. [16]. A separate calculation in which we added a subset of 20 pseudostates with $l=4$ produced only a minor change (of an order of a percent) for the ionization probabilities.

The initial conditions for the solution of the TDSE are determined by solving an eigenvalue problem using a subset of basis functions of the *S* symmetry only. This produced the ground-state energy of −2.903 30 a.u. We integrate the TDSE up to a time $T_1$ when the external field is switched off. Then we project the solution onto a field-free CCC wave function $\Psi(\mathbf{k}_1,\mathbf{k}_2)$ representing two electrons in continuum. Details of the construction of these functions can be found, for example, in Ref. [28] or in our earlier paper [16].

A set of the final states corresponding to various photoelectron energies $E_1$ and $E_2$ was prepared. The energies $E_1$ and $E_2$ were taken on a grid $E_i=1,4,7,10,13,16,19,22,27,40,100,200$ eV. Projection of the solution of the TDSE on the states of this grid gives us a probability distribution function $p(\boldsymbol{k}_1,\boldsymbol{k}_2)$ of finding the helium atom in a field-free two-electron continuum state $\boldsymbol{k}_1,\boldsymbol{k}_2$ at the time $t=T_1$.

From this probability, we can compute various differential and the total integrated cross sections of TPDI. The fully resolved, with respect to the photoelectron angles and their energy, triple-differential cross section (TDCS) is defined as

$$\frac{d\sigma(\omega)}{dE_1 d\Omega_1 d\Omega_2} = \frac{C}{W q_1 q_2 \cos^2\alpha}\int p(\boldsymbol{k}_1,k_1\tan(\alpha)\tilde{\boldsymbol{k}}_2)k_1 dk_1. \tag{9}$$

The total integrated cross section (TICS) is computed as

$$\sigma(\omega) = \frac{C}{W}\int p(\boldsymbol{k}_1,\boldsymbol{k}_2)d\hat{\boldsymbol{k}}_1 d\hat{\boldsymbol{k}}_2 dk_1 dk_2. \tag{10}$$

Here $W=\int_0^{T_1}F_{\rm ac}^4(t)dt$ and $C=12\pi^2 a_0^4\tau\omega^2c^{-2}$ is the TPDI constant expressed in terms of the speed of light in atomic units $c\approx 137$, Bohr radius $a_0=0.529\times 10^{-8}$ cm, and atomic unit of time, $\tau=2.418\times 10^{-17}$ s. The momenta $q_1$ and $q_2$ in Eq. (9) are defined on the energy shell: $E_1=q_1^2/2$, $E-E_1=q_2^2/2$, $\tan\alpha=q_2/q_1$, where $E$ is the excess energy.

## III. RESULTS

Before presenting our numerical TICS results across the studied photon energy range, we wish to outline the procedure we use to attest the accuracy of our calculation.

### A. Accuracy of the calculation

The fact that the wave functions on which we project the solution of the TDSE and the basis set used to solve the TDSE are two unrelated sets of functions may produce considerable inaccuracy in the calculated probabilities. An obvious requirement which a numerically reliable calculation must satisfy is independence of the computed probabilities on time for times larger than the time $T_1$ when the ac field is completely switched off.

Let us consider the time evolution of the helium atom in the absence of an ac external field. This evolution can be presented as a sum

$$\Psi(t) = \sum c_k e^{-iE_k t}\Psi_k, \tag{11}$$

where $\Psi_k$ and $E_k$ are solutions of the eigenvalue problem for the field-free helium Hamiltonian on the basis (7). The eigenvectors $\Psi_k$ are not strictly orthogonal to the CCC field-free states. The overlap of the solution of the TDSE and CCC states will therefore contain terms $\Sigma c_k e^{-iE_k t}\langle\Psi_{\rm CCC}|\Psi_k\rangle$. These terms introduce beats in the computed probabilities which may affect the accuracy of the calculation considerably unless the overlaps $\langle\Psi_{\rm CCC}|\Psi_k\rangle$ peak in a narrow range of energies $E_k$. The magnitude of these beats may serve as an indicator of the accuracy of the calculation.

This point is illustrated in Fig. 1 where we plot the squared overlaps $|\langle\Psi_{\rm CCC}|\Psi_k\rangle|^2$ between various $D$-symmetry eiegenfunctions of the eigenvalue problem for the field-free helium Hamiltonian on the basis (7) and a final-state CCC wave function at excess energy of 20 eV above the double-ionization threshold. We see that indeed there are only a few leading overlaps which peak narrowly around this energy and other overlaps are insignificant on this scale.

Narrow localization of the overlaps on the energy scale dampens the beats considerably. This is illustrated in the Table I where we present the partial $D$- and $S$-wave contributions to the TICS computed for several selected photon energies. These data are obtained as follows. The first set of TICS (second and sixth columns) is computed by overlapping the solution of the TDSE and the CCC wave functions at the time $T_2=T_1=6\,T$ when the ac field is switched off. To obtain the second set of data (third and seventh columns), we let the atom evolve freely for one period after the ac field is switched off and then the overlaps with the CCC field free states are computed at the moment $T_2=7T$. The data from the fourth and eighth columns have been obtained when the system evolves freely for two periods of the ac field after it is switched off and the overlaps are computed at the moment $T_2=8T$. As one can see from these data, the beats mentioned above lead to variations of the TICS of the order of 20% for the photon energy range covered in Table I.

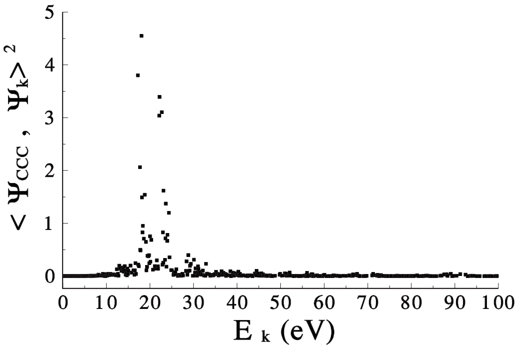

FIG. 1. Squared overlaps $|\langle\Psi_{\rm CCC}|\Psi_k\rangle|^2$ between various $D$-symmetry eiegenfunctions of the eigenvalue problem for the field-free helium Hamiltonian on the basis (7) and a CCC wave function at the excess energy of 20 eV above the double-ionization threshold.

This issue of the time dependence of the computed probabilities for times larger than $T_1$, when the laser field is switched off, is closely related to a problem discussed in Ref. [13]. The use of different quantum mechanical pictures (e.g., the Schrödinger or interaction one) may give different results for the ionization probabilities. The mathematical origin of this phenomenon is exactly the same as the origin of the beats discussed above.

Indeed, let $\hat{B}$ be a projecting operator on a subset of the final states (doubly ionized in the present context) in the Schrödinger picture. Let $\Psi(T_1)$ be the Schrödinger wave function describing an atomic state at the moment $t=T_1$ when the atom–ac-field interaction is completely switched off. After the moment of time $T_1$, the atom evolves freely and the probability $P_S$ to find the atom at the moment $t>T_1$ in any of the states belonging to the range of the projection operator $\hat{B}$ is

$$P_S(t) = \langle\Psi(T_1)|e^{i\hat{H}_{\rm atom}(t-T_1)}\hat{B}e^{-i\hat{H}_{\rm atom}(t-T_1)}|\Psi(T_1)\rangle, \tag{12}$$

where $\hat{H}_{\rm atom}$ is the Hamiltonian of the atom. If we had in our disposal the exact eigenstates of $\hat{H}_{\rm atom}$ describing doubly ion-

TABLE I. Partial $D$- and $S$-wave contributions to the TICS, in units of $10^{-52}$ cm$^4$ s, obtained for values of $T_2=6T$, $7T$, $8T$ and in the interaction picture.

| | $D$-wave | | | | $S$-wave | | | |
|---|---|---|---|---|---|---|---|---|
| $\omega$ | $6T$ | $7T$ | $8T$ | I | $6T$ | $7T$ | $8T$ | I |
| 42 | 0.500 | 0.443 | 0.506 | 0.615 | 0.136 | 0.120 | 0.216 | 0.071 |
| 45 | 0.962 | 0.775 | 0.959 | 0.801 | 0.233 | 0.279 | 0.390 | 0.301 |
| 48 | 1.459 | 1.298 | 1.374 | 1.307 | 0.424 | 0.610 | 0.593 | 0.512 |
| 50 | 1.646 | 1.768 | 1.629 | 1.582 | 0.321 | 0.428 | 0.283 | 0.367 |

ized states, we could built the projection operator $\hat{B}$ from these states. Such a projection operator would commute with $\hat{H}_{\text{atom}}$ in Eq. (12) and the probability $P_S$ defined by this equation would be time independent. Since we have only approximate expressions for the wave functions from which we build the projector $\hat{B}$, the probability defined by Eq. (12) is, in fact, a function of time. This brings us back to the time-beat phenomenon which we discussed above. On the other hand, in the interaction picture, the probability to find the atom in any of the states belonging to the range of the projection operator $\hat{B}$ at the moment $t=T_1$ is $P_I = \langle \Psi_I(T_1)|\hat{B}|\Psi_I(T_1)\rangle$, where $\Psi_I(T_1)$ is the interaction picture wave function describing atom at the moment $t=T_1$. Projection operators which are presumed to be built from the exact eigenstates of $\hat{H}_{\text{atom}}$ coincide in both pictures. Using the connection $\Psi_I(T_1)=e^{i\hat{H}_{\text{atom}}T_1}\Psi(T_1)$ between vectors in the two pictures, we will obtain an equation similar to Eq. (12) where we should put $t=0$ in arguments of the exponential functions. Again, we see that if we had in our disposal the exact eigenfunctions of $\hat{H}_{\text{atom}}$, describing doubly ionized states of a field-free atom, we would get identical answers in both pictures. As was emphasized in [13], the origin of the nonequivalence of the two quantum mechanical pictures lies in the fact that we use approximate wave functions for the projection operator.

The accuracy check performed above is, therefore, equivalent to the comparison of the results given by the two pictures which was used as an accuracy check in papers [13,17]. In the framework of our time-beat test, we can also make a direct comparison of the results given by the two pictures. This can be achieved by taking a Schrödinger wave function at the moment $T_1$ and propagating it backwards in time to the moment $t=0$ using the field-free atomic Hamiltonian $H_{\text{atom}}$. Projecting the resulting wave function on a manifold of the CCC states will give us an interaction picture result. Corresponding data are presented in Table I (columns 5 and 9). The deviation of these data from the results obtained in the Schrödinger picture is of the order of 20% in the total cross section, confirming the accuracy estimate based on the time-beat test.

All the discussion given so far in this section applies to the case when the only source of time beats (or nonequivalence of different quantum mechanical pictures of motion) lies in the fact that the final states on which we project the solution of the TDSE are not the exact eigenstates of the atomic Hamiltonian. Since the basis used for the solution of the TDSE is necessarily finite, it does not cover the whole Hilbert space. If $\hat{A}$ is a projection operator on a linear hull of all basis vectors used for the solution of the TDSE [all linear combinations of vectors given by Eq. (7) in our case], then the TDSE we are solving is not $i\partial\Psi/\partial t=\hat{H}\Psi$ but rather $i\partial\Psi/\partial t=\hat{A}\hat{H}\hat{A}\Psi$. This means, for example, that in the formulas given above we should use the operator $\hat{A}\hat{H}_{\text{atom}}\hat{A}$ rather than $\hat{H}_{\text{atom}}$. Correspondingly, other operators are also to be modified. Usually, however, one can make the projection operator $\hat{A}$ very close to an identity operator by choosing a large enough basis.

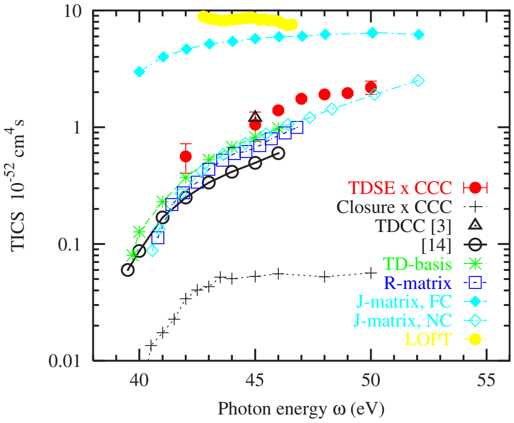

FIG. 2. (Color online) Total integrated cross section of TPDI on He as a function of the photon energy. Present results obtained by combination of the TDSE and CCC methods and corresponding to a field intensity of $3.5\times10^{14}$ W/cm$^2$ are shown by red solid circles. The CCC calculation in the closure approximation [30] is shown by black crosses. Other calculations are as follows: TDCC with a sin$^2$ envelope, $5\times10^{14}$ W/cm$^2$ [15], open circles; TDCC with a ramped pulse, $10^{14}$ W/cm$^2$ [6], open triangle; time-dependent (TD) basis, $10^{14}$ W/cm$^2$ [8], green asterisks; $R$ matrix, $10^{13}$ W/cm$^2$ [5], blue open squares; $J$ matrix with noncorrelated (NC) and correlated (FC) final states, $10^{13}$ W/cm$^2$ [13], light blue open and solid diamonds, respectively; LOPT [3], yellow solid circles.

For energies outside the photon frequency range presented in Table I, the TICS results are fluctuating much more and, hence, are considerably less reliable. This can probably be explained if we recall the nature of the beats in the computed probabilities. Their magnitude is determined eventually by the spectrum of the eigenvalue problem for the field-free helium Hamiltonian in basis (7) and the set of CCC final-state wave functions we use. Proceeding further into a domain of larger frequencies probably requires additional tuning of both sets.

### B. Total integrated cross section

In Fig. 2, we present our results for TICS in the whole photon energy range from 42 to 50 eV studied in the paper. The "error bars" attached to our data indicate the fluctuation of the TICS due to free propagation beats. In Fig. 2, we compare the present calculation with known literature values obtained by the following methods: TDCC [6,15], $R$ matrix [5], time-dependent basis [8], $J$ matrix [13], and LOPT [3].

As we have already mentioned in the Introduction, the overall picture is anything but simple. In the photon energies interval of 42–47 eV, our TICS values lie close to the results of the TDCC approach [6,15] and the $R$-matrix Floquet method [5]. For larger energies, outside the interval studied in Refs. [5,6,15], our calculation suggests that the TICS, as a function of photon energy, flattens and may have a maximum in the vicinity of 50 eV. This shape of energy dependence of the TICS is quite similar to that found in Ref. [13]. However, their magnitude of the TICS is several times larger.

In Fig. 2 we also present our earlier CCC calculation in the closure approximation [31] which produced the TICS

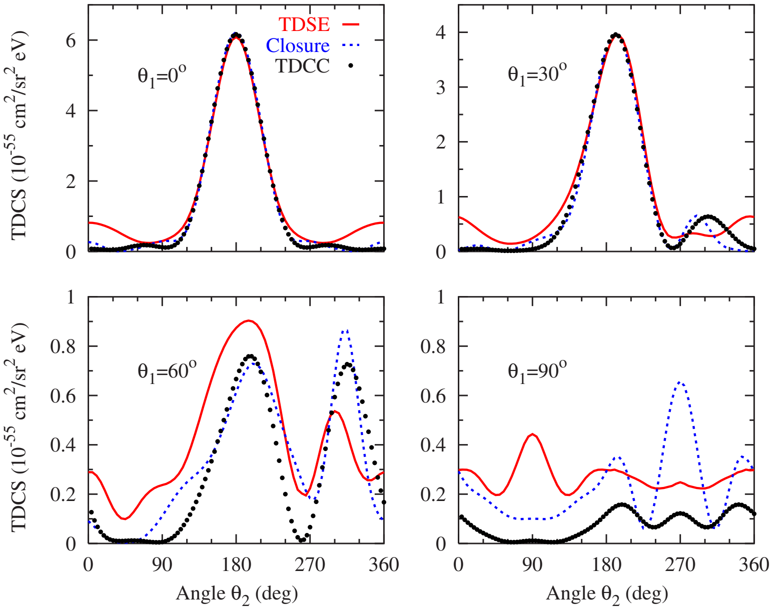

FIG. 3. (Color online) TDCS of He TPDI for the coplanar geometry at $\omega = 42$ eV, $E_1 = E_2 = 2.5$ eV, and various fixed electron angles. The present TDSE calculation (divided by 2.2) is shown by the red solid line. The earlier CCC calculation in the closure approximation (divided by 1.6) is shown by the blue dashed line. The black dots represent the TDCC results of Ref. [15].

values far below all other reported results. In our earlier calculation, we employed the LOPT with respect to the field-atom interaction whereas the final-state electron correlation was included in full. In addition, all the intermediate states of the atom between absorption of the first and second photons were weighted equally and the infinite spectral sum was taken using the closure relation. Thus, the abnormally small TICS values obtained in Ref. [31] could be attributed either to the inability of LOPT to describe adequately the physical situation or failure of the closure approximation itself.

The possibility of a perturbative treatment of the field-atom interaction in TPDI of He was studied by several authors. The results of Ref. [6] indicated that nonperturbative effects might play a very considerable role at photon frequencies around 45 eV and for ac field strength of the order of 0.1 a.u. On the other hand, the LOPT calculation of Ref. [3] produced results in fair agreement with a nonperturbative calculation of Ref. [13] as well as the subsequent time-dependent calculation of the same authors [14]. Our own preliminary and unpublished LOPT calculation based on the Kramers-Henneberger picture of the atom-laser field interaction [32] showed that a perturbative treatment may still be possible for field intensities of the order of 0.1 a.u.

We therefore tend to attribute the failure of our earlier calculation [30] to produce sensible TICS values to the closure approximation or the wrong choice of the average energy denominator. This calculation was nevertheless useful as it generated quite reasonable angular correlation patterns in the two-electron continuum. This issue will be discussed in the next section.

### C. Fully differential cross section

In Fig. 3, we present our results for the fully resolved TDCS of TPDI of He at the photon energy of 42 eV and the equal energy sharing between two photoelectrons $E_1 = E_2 = 2.5$ eV. We adopt the coplanar geometry in which the momenta of the two photoelectrons and the polarization vector of light belong to the same plane which is perpendicular to the propagation direction of the photon. We compare the present TDSE results with our earlier CCC calculation in the closure approximation [31]. In Fig. 3 we also present the TDCC results of Hu *et al.* [15]. To make a shape comparison, we divide the present calculation by the same factor of 2.2 for all fixed electron angles. This factor reflects the difference in the TICS between the two methods.

There is a good shape agreement between the three sets of calculations for the fixed photoelectron angles of $\theta_1 = 0°$ and 30°. This agreement deteriorates somewhat at $\theta_1 = 60°$ and breaks down for $\theta_1 = 90°$. Partial-wave analysis of the TDCS shows that the *D*-wave contribution is very similar in the three calculations for all angles. However, the relative strength of the *S* and *D* waves is somewhat different which manifests itself at larger fixed electron angles where the *S*-wave contribution becomes noticeable.

We notice that in the perturbative closure calculation [31] and the present time-dependent calculation, we employ the same CCC final state whereas the theoretical description of the field-atom interaction is different. As was mentioned in the preceding section, these two calculations give different values of the TICS. However, the overall shapes of the TDCS are fairly similar. This fact indicates that the energy and angular correlations in the two-electron continuum are established as the result of the electron correlation in the final doubly ionized state. This correlation takes place at large times (and distances) when the pulse of the electromagnetic field is already switched off. That is why it shows little sensitivity to the precise mechanism of the atom-field interaction.

## IV. CONCLUSION

In the present work, we studied two-photon double electron ionization of helium in the range of photon energies from 42 to 50 eV. We employed a nonperturbative time-dependent approach to describe the interaction of the atom with the electromagnetic field. The correlation in the final doubly ionized state was accounted for by the convergent close-coupling method.

As far as the total integrated cross section is concerned, our calculation seems to be much closer to a group of results presented in Refs. [5,6,8,15] rather than to the recent calculations of Ref. [13,14]. Our calculation also deviates, in both magnitude and shape of the photon energy dependence, from the perturbative calculation of Ref. [3].

As we mentioned in the Introduction, an attempt to explain this clustering of theoretical data by categorizing them with respect to account or neglect of the final-state correlation does not seem to clear the situation. As we noted, the uncorrelated final-state calculation of Ref. [6] agrees well the correlated calculation of Ref. [5] and the present calculation. It was noted in Refs. [3,13] that neglect of correlations in the final state tends to diminish the TICS. A particularly striking demonstration of this effect was given in [13], where the switching off the correlations brought the *J*-matrix results to a good agreement with Ref. [5] and, consequently, to the present results (see Fig. 2).

Given a large spread of reported data, more work needs to be done before the values of the TICS are firmly established as is presently the case for single-photon double ionization. The decisive role in resolving this issue may be played by the experiment. In a recent experimental work [33], the authors reported TICS values between $2\times10^{-52}$ and $2.9\times10^{-52}$ cm$^4$ s for a photon energy of 41.8 eV, which is rather close to the results of Ref. [13].

## ACKNOWLEDGMENTS

We wish to thank James Colgan for supplying the data in numerical form. The authors acknowledge support of the Australian Research Council in the form of Discovery Grant No. DP0451211. Facilities of the Australian Partnership for Advanced Computing (APAC) were used.

[1] M. Protopapas, C. H. Keitel, and P. L. Knight, Rep. Prog. Phys. **60**, 389 (1997).
[2] A. Becker, R. Dörner, and R. Moshammer, J. Phys. B **38**, S753 (2005).
[3] L. A. A. Nikolopoulos and P. Lambropoulos, J. Phys. B **34**, 545 (2001).
[4] T. Mercouris, C. Haritos, and C. A. Nicolaides, J. Phys. B **34**, 3789 (2001).
[5] L. Feng and H. W. van der Hart, J. Phys. B **36**, L1 (2003).
[6] J. Colgan and M. S. Pindzola, Phys. Rev. Lett. **88**, 173002 (2002).
[7] G. L. Kamta and A. F. Starace, Phys. Rev. A **65**, 053418 (2002).
[8] B. Piraux, J. Bauer, S. Laulan, and H. Bachau, Eur. Phys. J. D **26**, 7 (2003).
[9] P. Lambropoulos, P. Maragakis, and J. Zhang, Phys. Rep. **305**, 203 (1999).
[10] A. Scrinzi and B. Piraux, Phys. Rev. A **58**, 1310 (1998).
[11] J. Caillat, J. Zanghellini, M. Kitzler, O. Koch, W. Kreuzer, and A. Scrinzi, Phys. Rev. A **71**, 012712 (2005).
[12] M. S. Pindzola and F. Robicheaux, J. Phys. B **31**, L823 (1998).
[13] E. Foumouo, G. L. Kamta, G. Edah, and B. Piraux, Phys. Rev. A **74**, 063409 (2006).
[14] L. A. A. Nikolopoulos and P. Lambropoulos, J. Phys. B **40**, 1347 (2007).
[15] S. X. Hu, J. Colgan, and L. A. Collins, J. Phys. B **38**, L35 (2005).
[16] I. A. Ivanov and A. S. Kheifets, Phys. Rev. A **74**, 042710 (2006).
[17] S. Laulan and H. Bachau, Phys. Rev. A **68**, 013409 (2003).
[18] A. Becker and F. H. M. Faisal, J. Phys. B **38**, R1 (2005).
[19] C. W. McCurdy, T. N. Rescigno, and D. Byrum, Phys. Rev. A **56**, 1958 (1997).
[20] M. Baertschy, T. N. Rescigno, and C. W. McCurdy, Phys. Rev. A **64**, 022709 (2001).
[21] C. W. McCurdy, D. A. Horner, T. N. Rescigno, and F. Martin, Phys. Rev. A **69**, 032707 (2004).
[22] M. Pont and R. Shakeshaft, Phys. Rev. A **51**, 494 (1995).
[23] S. Laulan, H. Bachau, B. Piraux, J. Bauer, and G. L. Kamta, J. Mod. Opt. **50**, 353 (2003).
[24] L. Malegat, P. Selles, and A. K. Kazansky, Phys. Rev. Lett. **85**, 4450 (2000).
[25] J. Colgan and M. S. Pindzola, J. Phys. B **37**, 1153 (2004).
[26] J. Colgan and M. S. Pindzola, Phys. Rev. Lett. **88**, 173002 (2002).
[27] I. Bray, Phys. Rev. A **49**, 1066 (1994).
[28] I. Bray and A. T. Stelbovics, Adv. At., Mol., Opt. Phys. **35**, 209 (1995).
[29] D. V. Fursa and I. Bray, J. Phys. B **30**, 757 (1997).
[30] I. A. Ivanov and A. S. Kheifets, Eur. Phys. J. D **38**, 249 (2006).
[31] A. S. Kheifets and I. A. Ivanov, J. Phys. B **39**, 1731 (2006).
[32] I. A. Ivanov and A. S. Kheifets, J. Phys. B **38**, 2245 (2005).
[33] H. Hasegawa, E. J. Takahashi, Y. Nabekawa, K. L. Ishikawa, and K. Midorikawa, Phys. Rev. A **71**, 023407 (2005).